Bioorganic & Medicinal Chemistry Letters 20 (2010) 469–473

Contents lists available at ScienceDirect

Bioorganic & Medicinal Chemistry Letters

journal homepage: www.elsevier.com/locate/bmcl

Continued exploration of the triazolopyridine scaffold as a platform for p38 MAP kinase inhibition

Kevin D. Jerome [a,*], Paul V. Rucker [a,†], Li Xing [a], Huey S. Shieh [a], John E. Baldus [a], Shaun R. Selness [a], Michael A. Letavic [b,‡], John F. Braganza [b,§], Kim F. McClure [b]

[a] Pfizer Global Research and Development, St. Louis Laboratories, 700 Chesterfield Pkwy. W., Chesterfield, MO 63017, USA
[b] Pfizer Global Research and Development, Groton Laboratories, Eastern Point Road, Groton, CT 06340, USA

ARTICLE INFO

Article history:
Received 4 September 2009
Revised 20 November 2009
Accepted 23 November 2009
Available online 26 November 2009

Keywords:
p38
Kinase
Triazolopyridines

ABSTRACT

The structure based drug design, synthesis and structure–activity relationship of a series of C6 sulfur linked triazolopyridine based p38 inhibitors are described. The metabolic deficiencies of this series were overcome through changes in the C6 linker from sulfur to methylene, which was predicted by molecular modeling to be bioisosteric. X-ray of the ethylene linked compound **61** confirmed the predicted binding orientation of the scaffold in the p38 enzyme.

Inhibition of the p38α mitogen-activated protein (MAP) kinase as a viable drug target has garnered a great deal of attention from multiple drug companies and academic institutions worldwide.[1] MAP protein kinase p38 is a dual specificity kinase that has four known isoforms (α, β, γ, and δ), with their expression varying amongst cell types of the immune system; and p38α being the chief isoform implicated in inflammatory disease.[2] To date there are now over half a dozen US approved kinase inhibitors, but none yet approved that specifically target p38 as a mediator of inflammatory cytokines. Preclinical studies strongly support that selective inhibition of p38α can effectively modulate tumor necrosis factor (TNF-α), interleukin-1β (IL-1β) and other cytokine production. Because TNFα and IL-1β have been implicated as key cytokines in inflammatory diseases, p38 has been pursued as a kinase target for such diseases as rheumatoid arthritis (RA), Crohn's disease, inflammatory bowel syndrome (IBS), and psoriasis.[3] One current treatment option for these inflammatory diseases is with biological agents known for shutting down TNF-α function with great success.[4] Hence it is anticipated that a small molecule p38α MAP kinase inhibitor should provide therapeutic value for the treatment of such inflammatory conditions.

Our strategy has been similar to those employed by other organizations in the search for novel p38 MAP kinase inhibitors: (1) determine a privileged scaffold that provides potent compounds and permits the construction of an SAR grid, (2) build in drug-able properties that will drive both in vitro potency and in vivo exposure, (3) identify key functionality that imparts kinase selectivity.

In earlier reports from our organization, we disclosed such a scaffold targeting p38α, manifested in the oxazole substituted triazolopyridine chemotype **1**.[5] In addition, many other p38 inhibitors have been reported in the literature, including VX-745.[6] Herein we report our current progress with the triazolopyridine series, specifically around the replacement of the oxazole functionality with a series of isosteric linear chains.

Structure-based design was used to combine key binding elements of the triazolopyridine compound CP-808844 **1** and VX-745 **2** to design compound **3**, utilizing a C6 sulfur atom linker as an oxazole bioisosteric replacement (Fig. 1).

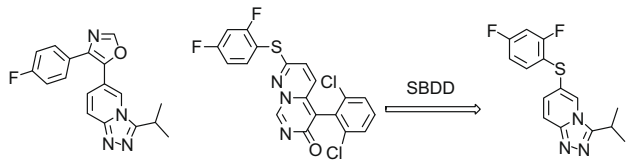

Figure 1. Structure based drug design of C6 sulfur linked triazolopyridines from CP-808844 (**1**) and VX-745 (**2**).

* Corresponding author. Tel.: +1 636 247 8655; fax: +1 636 247 0966.
E-mail address: kevin.d.jerome@pfizer.com (K.D. Jerome).
† Present address: Genomics Institute of the Novartis Research Foundation (GNF), 10675 John Jay Hopkins Dr., San Diego, CA 92121, USA.
‡ Present address: Johnson & Johnson PRD-La Jolla, 3210 Merryfield Row, San Diego, CA 9212, USA.
§ Present address: Pfizer Global Research and Development, La Jolla Laboratories, 10770 Science Center Drive, San Diego, CA 92121, USA.

0960-894X/$ - see front matter © 2009 Elsevier Ltd. All rights reserved.
doi:10.1016/j.bmcl.2009.11.114

The synthesis of the initial bromo triazolopyridine scaffold was achieved through two different routes. In both routes, the initial step required the conversion of the di-bromo pyridine, **4**, to the hydrazine, **5**, which afforded solely the regioisomer shown (Scheme 1). In Method A, a one pot synthesis of the bromo triazolopyridine core was achieved by acylation of **5** to give the in situ formation of the corresponding hydrazide, followed by dehydration to the triazolopyridine.[7]

Method B shows an alternate two step synthesis of the bromo triazolopyridine core from the hydrazine, **5**. Acylation of **5** formed the hydrazide, which was isolated, followed by dehydration to the triazolopyridine. Although Method B contains an additional synthetic step, it was found to be more general than the one pot route in Method A. The bromo triazolopyridine cores synthesized, **6–15**, as well as the method used to synthesize them, are shown in Table 1.

The sulfur linked triazolopyridines were synthesized from the bromo triazolopyridine cores, **6–15**, and various aryl disulfide compounds. These aryl disulfides were synthesized by two methods. The initial method (Scheme 2) involved the dimerization of 2,4-difluorophenyl thiol using neutral alumina[8] to form the disulfide **16**.

The preparation of additional aryl disulfides was accomplished through a method that permitted the use of the more commercially abundant sulfonyl chlorides, using WCl_6 and NaI to provide their corresponding disulfides (Scheme 3, Table 2).[9]

Aryl disulfides **16–19** were then allowed to react with the corresponding Grignards derived from **6 to 15** (Scheme 4, Table 3). The HCl salt of the triazolopyridine could be formed by treatment

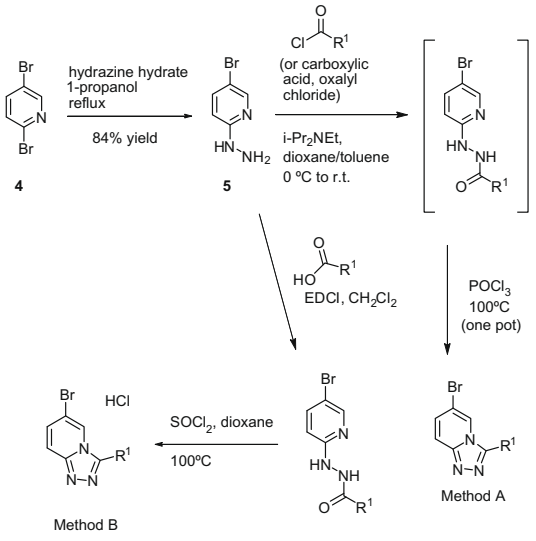

Scheme 1. Alternate syntheses of the bromo triazolopyridine Scaffold.

Table 1
Bromo triazolopyridine cores

Compounds	R^1	Method
6	*iso*-Propyl	A
7	*t*-Butyl	A
8	1-Methylcyclopropyl	B
9	2-Methylpent-4-en-2-yl	A
10	2,6-DiF-Ph	A
11	2-Me-4-Br-Ph	A
12	3-COOMe-Ph	B
13	2-Me-5-COOMe-Ph	A
14	4-COOMe-Ph	B
15	4-Piperidine	B

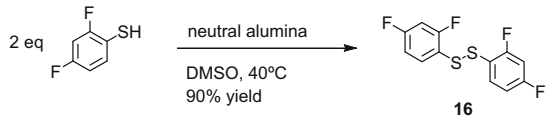

Scheme 2. Synthesis of aryl disulfides from thiols.

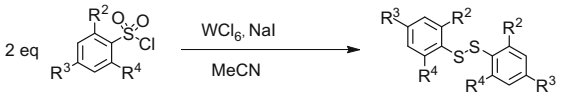

Scheme 3. Synthesis of aryl disulfides from sulfonyl chlorides.

Table 2
Aryl disulfides from sulfonyl chlorides

Compounds	R^2	R^3	R^4	Yield (%)
17	CF_3	Br	H	82
18	CF_3	F	H	79
19	Cl	Cl	Cl	77

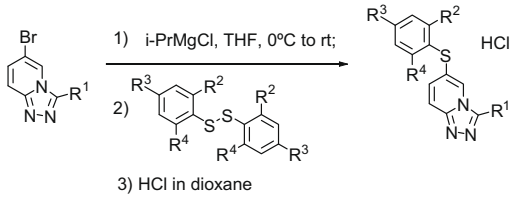

Scheme 4. Synthesis of sulfur linked triazolopyridines.

with 4 N HCl in dioxane following work-up. If the starting bromo triazolopyridine core was an HCl salt, 2 equiv of Grignard reagent were necessary.

Triazolopyridine cores, **9** and **11–14**, were further elaborated, using known chemistry, to obtain additional compounds shown in Table 3. Although the sulfur linked triazolopyridines afforded some single digit nM inhibitors of p38α, the series as a whole suffered from a poor metabolic and pharmacokinetic profile. However, **3** did show p38α inhibition of 79 nM, had 89% human liver and 46% rat liver microsomal stability[10] and was the only compound in the series to show significant in vivo activity (61% inhibition of rat LPS@ 5 MPK, 4 h).[11] Therefore, **3** was considered as validation that a linear linkage could potentially substitute for the oxazole in a potent triazolopyridine p38α inhibitor, warranting further study to improve metabolic stability and p*K* properties, and ultimately the in vivo activity of the series.

It was determined through metabolic identification experiments that the most prevalent metabolic soft spot was oxidation of the sulfur linkage to the sulfoxide and/or the sulfone. It was hypothesized that if bulky groups were installed to C5 and C7 of the triazolopyridine core of **3**, the sulfur atom would be sterically shielded and thereby metabolism would be blocked. Based on modeling studies, the C5 carbon of the triazolopyridine would be well tolerated for substitution. In contrast, substitution of the C7 position would interfere with the binding conformation of the 2,4-difluorophenyl group towards the lipophilic pocket of p38α.

Triazolopyridine **3** was halogenated[12] (Fig. 2) to obtain the modeled analogs. Consistent with the predictions by molecular modeling, compound **48** showed good p38α activity (Table 4), and any substitution at R^6 (C7 of the triazolopyridine) resulted in loss of activity.

Table 3
Sulfur linked triazolopyridines

Compd	Core	Disulfide	R^1	R^2	R^3	R^4	p38α IC_{50} (nM)
3	6	16	*i*-Pr	F	F	H	79.3
20	7	16	*t*-Bu	F	F	H	4.8
21	8	16	1-Me-cyclopropyl	F	F	H	24.9
22	9	16	2-Me-pent-4-en-2-yl	F	F	H	16.3
23	9	16	1,1-DiMe-3,4-butanediol	F	F	H	1740
24	10	16	2,4-Diflurophenyl	F	F	H	7.2
25	11	16	2-Me-4-Br-phenyl	F	F	H	141
26	11	16	2-Me-4-vinyl-phenyl	F	F	H	106
27	11	16	2-Me-4-(1,2-diOH·Et)-Ph	F	F	H	28.3
28	11	16	2-Me-4-(CH_2NH-(CH_2)$_2$OH-Ph	F	F	H	33.3
29	12	16	3-COOMe-phenyl	F	F	H	181
30	12	16	3-COOH-phenyl	F	F	H	7420
31	12	16	3-$CONH_2$-phenyl	F	F	H	241
32	13	16	2-Me-5-COOMe-phenyl	F	F	H	7.8
33	13	16	2-Me-5-COOH-phenyl	F	F	H	2920
34	13	16	2-Me-5-$CONH_2$-phenyl	F	F	H	60.8
35	13	16	2-Me-5-CONHMe-Ph	F	F	H	39.9
36	13	16	2-Me-5-$CONHCH_2$-CONH2-Ph	F	F	H	46.5
37	13	16	2-Me-5-CONH(CH_2)$_2$-OH-phenyl	F	F	H	20.5
38	14	16	4-COOMe-Ph	F	F	H	322
39	14	16	4-COOH-Ph	F	F	H	1170
40	14	16	4-$CONH_2$-Ph	F	F	H	201
41	14	16	4-CONHMe-Ph	F	F	H	293
42	15	16	4-Piperidine	F	F	H	3770
43	15	16	*N*-$COCH_2$OAc-4-piperidine	F	F	H	367
44	15	16	*N*-$COCH_2$OH-4-piperidine	F	F	H	212
45	6	17	*i*-Pr	CF_3	Br	H	>10,000
46	6	18	*i*-Pr	CF_3	F	H	>10,000
47	6	19	*i*-Pr	Cl	Cl	Cl	8240

Human and rat liver microsomal data showed that the halogenation hypothesis failed to improve upon the metabolic stability of the compounds. At this point, we sought to replace the sulfur linkage altogether with an alternative connection that might afford better in vivo stability. Given the large size of the sulfur atom and the flexibility of the sulfur–carbon bond, the distance afforded by the sulfur linker is suggested to be between that of a methylene and ethylene unit. Upon evaluating a number of alternative linkers by molecular modeling, based on their ability to maintain the relative binding conformations of the hinge binding core and the lipophilic aryl group, several triazolopyridine analogs were synthesized and tested for p38α potency and in liver microsomal stability assays (Fig. 3, Table 5).

In modeling studies, the methylene and ethylene linkers appeared to be a suitable replacement for sulfur. Upon evaluation, these replacements gave potent p38α inhibition, with **57** and **58** showing similar p38α potency as **3**. Compound **57** in particular also showed a very favorable metabolic stability profile and therefore stood out as the most promising sulfur replacement linker.

On the other hand, from modeling studies the ketone moiety appeared too rigid, imposing a restricted conformation of the 2,4-difluorophenyl that disrupted its interaction with the aryl pocket. This hypothesis was supported, as **52** showed a significant drop in p38α potency. The amide function appeared to have to adopt a *cis* conformation in order to preserve the binding interactions, and such energy penalty is reflected in the loss of activity of **55**.

The loss of activity of the sulfonyl linker **54** cannot be explained by steric effects, since little conformational change was suggested

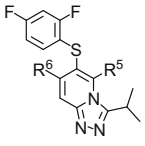

Figure 2. Halogenation of triazolopyridine **3**.

Table 4
Halogenated analogs of triazolopyridine 3

Compounds	R^5	R^6	P38α IC_{50} (nM)	HLM (% remaining)	RLM (% remaining)
3	H	H	79.3	89	46
48	Cl	H	12.3	65	23
49	H	Cl	889	71	37
50	Cl	Cl	3380	39	20
51	Br	Cl	6080	24	9

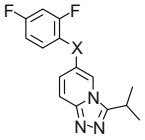

Figure 3. Alternate triazolopyridine bioisosteric linkers.

Table 5
Alternate triazolopyridine bioisosteric linkers

Compounds	X	P38α IC_{50} (nM)	HLM (% remaining)	RLM (% remaining)
3	S	79.3	89	46
52	C=O	1050	74	88
53	S=O	9680	100	100
54	SO_2	>10,000	ND	ND
55	(C=O)NH	>10,000	ND	ND
56	(C=O)CH_2	7370	ND	ND
57	CH_2	26.1	96	95
58	CH_2CH_2	85.0	53	54

from sulfur to sulfonyl and the protein sub-environment is open to accommodate the sulfonyl oxygen atoms. The effect could be electrostatic. One possibility is that the strong electron withdrawing sulfonyl group attenuates the hydrogen bond accepting ability of

the nitrogen atoms of the triazole. Such hydrogen bond recognition with the kinase hinge is critical for inhibitor potency, and is sensitive to the electron density distribution of the heterocyclic core.[13] Additionally, the sulfonyl oxygen atoms, each carrying a negative point charge and would interact unfavorably with the vicinal Asp168 on the p38α activation loop (O···O distance is ~4.2 Å per modeling). Both of the rationales would predict the potency trend observed for **3**, **53** and **54**, with the sulfoxide exhibiting an intermediate electrostatic property between the sulfur and the sulfonyl linkers. It was noted, however, that the metabolic stability of **53** was much improved over **3**.

Encouraged by our results from **57**, we continued to explore our options for the construction of carbon based bridges. The synthetic preparation of **61** is delineated in Scheme 5.[14] Conversion of bromide **59** to intermediate **60** was accomplished by conversion to the Grignard reagent using isopropyl magnesium chloride and subsequent trapping with DMF to provide the aldehyde. This aldehyde was then transformed into the ethylene bridge using a Wittig homologation and hydrogenation. The use of 2-chloro-4,6-dimethoxy-1,3,5-triazine as an activating agent to furnish the desired amide **61** provided slightly better overall yields than the conventional HATU coupling in this instance, owing to the insolubility of the acid precursor. The intermediate carboxylic acid was suspended in THF and treated with 4-methyl-morpholine followed by treatment with 2-chloro-4,6-dimethoxy-1,3,5-triazine. The resulting suspension was allowed to stir at room temperature followed by work-up with ammonium hydroxide and subsequent normal phase silica purification.[15]

Typified in Figure 4, we were able to utilize compound **61**, a potent p38α inhibitor of 40nM, by obtaining a co-crystal with the p38α enzyme.[16] The binary complex has been refined to 2.0 Å resolution with R_{work} = 23.6% (R_{free} = 27.5%) with good stereochemistry (rms deviation from ideality of 0.011 Å in bond lengths and 1.35° in bond angles). This co-crystallization permitted us to verify our binding model hypothesis and further demonstrate that carbon bridges, in this case ethylene, are sufficient substitutes for the sulfur atom linkage.

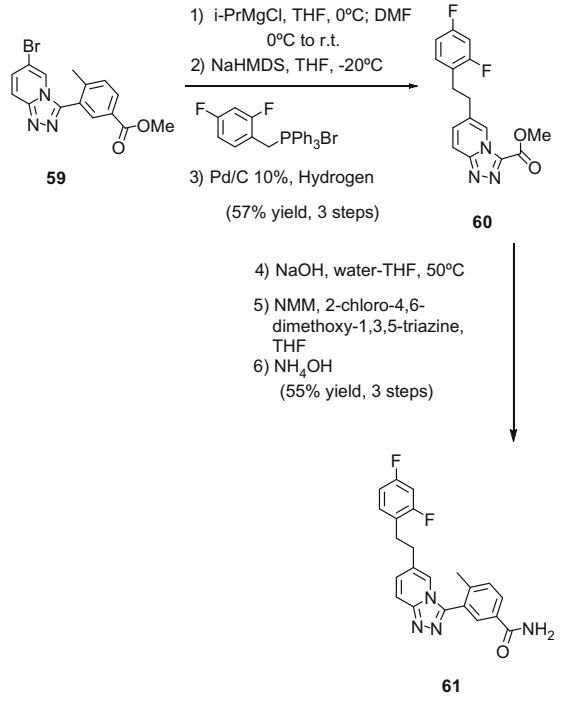

Scheme 5. Construction of triazolopyridine carbon atom linkages.

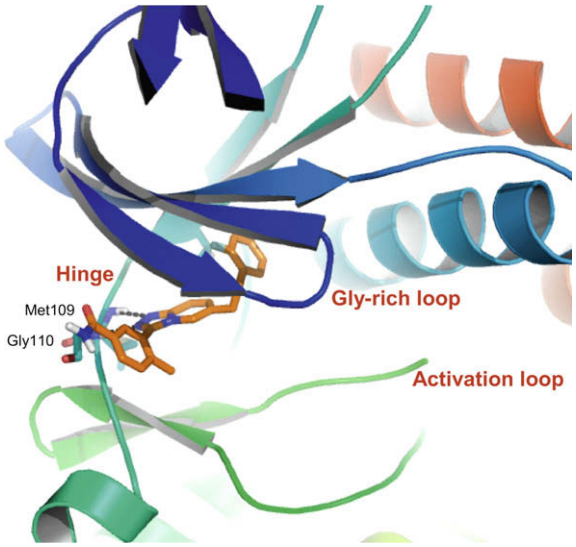

Figure 4. Crystal structure of compound **61** bound to p38α.

The crystal structure confirmed the binding models generated by molecular docking for the triazolopyridine compounds. As expected, **61** is bound at the ATP binding site of p38α kinase, which is located at the junction between the N- and C-terminal domains. The following protein residues define the binding site of **61**: the glycine-rich loop (31–38), the crossover peptide (107–111), C-terminal end of a α-helix (61–78), a β-strand from the N-terminal domain (49–53) and a β-strand from the C-terminal domain (162–171) and a flexible loop (84–86). The triazolopyridine ring anchors to the hinge region, and due to the small gate residue T106, the 2,4-difluorophenyl ring is able to insert into the hydrophobic pocket formed by residues Val 38, Ala 51, His 107, Leu 108, Met 109 and Leu 167. The benzamide moiety is exposed to the solvent region. Consistent with inhibitor structures of other chemical classes, the peptide bond connecting Met109 and Gly110 exhibits a flipped conformation from its apo state for the formation of the bidentate hydrogen bond.[13] The 1,2-nitrogen atoms of the triazolopyridine core serve as hydrogen bond acceptors that receive protons from the backbone NH of Met109 and Gly110.

In summary, the evolution of C6 linkers of triazolopyridine p38α inhibitors was described. Using structure based design, sulfur linked compounds such as **3** were first modeled, then found to be potent p38α inhibitors, but they lacked sufficient metabolic stability. Shown to be bioisosteric through modeling, methylene linked inhibitors such as **57** were found to be not only potent in p38α, but also metabolically stable. An X-ray of the ethylene linked compound **61** confirmed the binding models for the triazolopyridine series.

References and notes

1. Dominguez, C.; Tamayo, N.; Zhang, D. *Exp. Opin. Ther. Pat.* **2005**, *15*, 801.
2. (a) Foster, M. L.; Halley, F.; Souness, J. E. *Drug News Perspect.* **2000**, *13*, 488; (b) Lee, J. C.; Laydon, J. T.; McDonnell, P. C.; Gallagher, T. F.; Kumar, S.; Green, D.; McNulty, D.; Blumenthal, M. J.; Heys, J. R.; Landvatter, S. W.; Strickler, J. E.; McLaughlin, M. M.; Siemens, I. R.; Fisher, S. M.; Livi, G. P.; White, J. R.; Adams, J. L.; Young, P. R. *Nature* **1994**, *372*, 739.
3. (a) Arend, W. P.; Dayer, J. M. *Arthritis Rheum.* **1990**, *33*, 305; (b) Firestein, G. S.; Alvaro-Gracia, J. M.; Maki, R. *J. Immunol.* **1990**, *144*, 3347; (c) Rutgeerts, P.; D'Haens, G.; Targan, S.; Vasiliauskas, E.; Hanauer, S. B.; Present, D. H.; Mayer, L.; Van Hogezand, R. A.; Braakman, T.; DeWoody, K. L.; Shaible, T. F.; Van Deventer, S. J. H. *Gastroenterology* **1999**, *117*, 761; (d) Ulfgren, A. K.; Andersson, U.; Engstrom, M.; Klareskog, L.; Maini, R. N.; Taylor, P. C. *Arthritis Rheum.* **2000**, *43*, 2391.
4. Enbrel is a marketed soluble TNF-α receptor and Remicade is marketed as a TNF-a antibody therapy: (a) Jarvis, B.; Faulds, D. *Drugs* **1999**, *57*, 945; Seymour,

H. E.; Worsley, A.; Smith, J. M.; Thomas, S. H. L. *Br. J. Clin. Pharmacol.* **2001**, *51*, 201; (b) Rutgeerts, P. J. *Aliment. Pharmacol. Ther.* **1999**, *13*, 9; For other clinical examples of p-38 map kinase inhibitors efficacy see: Ferraccioli, G. F. *Curr. Opin. Anti-Inflamm. Immunomodulat. Invest. Drugs* **2000**, *2*, 74.
5. McClure, K. F.; Letavic, M. A.; Kalgutkar, A. S.; Gabel, C. A.; Audoly, L.; Barberia, J. T.; Braganza, J. F.; Carter, D.; Carty, T. J.; Cortina, S. R.; Dombroski, M. A.; Donahue, K. M.; Elliott, N. C.; Gibbons, C. P.; Jordan, C. K.; Kuperman, A. V.; Labasi, J. M.; LaLiberte, R. E.; McCoy, J. M.; Naiman, B. M.; Nelson, K. L.; Nguyen, H. T.; Peese, K. M.; Sweeney, F. J.; Taylor, T. J.; Trebino, C. E.; Abramov, Y. A.; Laird, E. R.; Volberg, W. A.; Zhou, J.; Bach, J.; Lombardo, F. *Bioorg. Med. Chem. Lett.* **2006**, *16*, 4339.
6. Haddad, J. J. *Curr. Opin. Invest. Drugs* **2001**, *2*, 1070.
7. McClure, K. F.; Abramov, Y. A.; Laird, E. R.; Barberia, J. T.; Cai, W.; Carty, T. J.; Cortina, S. R.; Danley, D. E.; Dipesa, A. J.; Donahue, K. M.; Dombroski, M. A.; Elliott, N. C.; Gabel, C. A.; Han, S.; Hynes, T. R.; LeMotte, P. K.; Mansour, M. N.; Marr, E. S.; Letavic, M. A.; Pandit, J.; Ripin, D. B.; Sweeney, F. J.; Tan, D.; Tao, Y. *J. Med. Chem.* **2005**, *48*, 5728.
8. Hirano, M.; Yakabe, S.; Monobe, H.; Morimoto, T. *J. Chem. Res.* **1998**, 472.
9. Firouzabadi, H.; Karimi, B. *Synthesis* **1999**, 500.
10. Metabolic stability was assessed in vitro by incubating 2 μM test compound with human or rat liver microsomes, NADPH and buffer at 37 °C for 45 min and measuring percent compound remaining by a precipitation procedure followed by LC–MS analysis.
11. Compounds were pre-dosed in male Lewis rats at various time points prior to an iv challenge with lipopolysaccharide. Blood was drawn 1.5 h post-challenge and TNF-α levels were evaluated by ELISA. The Pfizer Institutional Animal Care and Use Committee reviewed and approved the animal use in these studies. The animal care and use program is fully accredited by the Association for Assessment and Accreditation of Laboratory Animal Care, International.
12. Compounds **48**–**50** were separated from a mixture of regioisomers, in poor yield, by treating **3** with NBS, dichloroacetic acid in 1,2-dichloroethane at 50 °C. Treating **49** with NBS, dibromoacetic acid in 1,2-dichloroethane at 50 °C gave **51**, also in modest yield.
13. (a) Xing, L.; Shieh, H. S.; Selness, S. R.; Devraj, R. V.; Walker, J. K.; Devadas, B.; Hope, H. R.; Compton, R. P.; Schindler, J. F.; Hirsch, J. L.; Benson, A. G.; Kurumbail, R. G.; Stegeman, R. A.; Williams, J. M.; Broadus, Z. W.; Monahan, J. B. *Biochemistry* **2009**, *48*, 6402; (b) Fitzgerald, C. E.; Patel, S. B.; Becker, J. W.; Cameron, P. M.; Zaller, D.; Pilounis, V. B.; O'Keefe, S. J.; Scapin, G. *Nat. Struct. Biol.* **2003**, *10*, 764.
14. (a) Full disclosure of chemistry methods is made in the following patents: Rucker, P. V.; Jerome, K. D.; Selness, S. R.; Baldus, J. E.; Xing, L. PCT Int. Appl. 2006, 141 p, WO 2006018735.; (b) Rucker, P. V.; Jerome, K. D.; Selness, S. R.; Baldus, J. E.; Xing, L. PCT Int. Appl. 2006, 161 p, WO 2006018727.
15. Kaminski, Z. J. *Synthesis* **1987**, *10*, 917.
16. The atomic coordinates for the X-ray structure of p38α in complex with **61** have been deposited in the RCSB: rcsb id code—RCSB055916; PDB code—3KF7.